

Higgs boson production in weak boson fusion at next-to-leading order

Edmond L. Berger* and John Campbell†

High Energy Physics Division, Argonne National Laboratory, Argonne, Illinois 60439, USA

(Received 22 March 2004; published 15 October 2004)

The weak boson fusion process for neutral Higgs boson production is investigated with particular attention to the accuracy with which the Higgs boson coupling to weak bosons can be determined at CERN Large Hadron Collider energies in final states that contain a Higgs boson plus at least two jets. Using fully differential perturbative matrix elements for the weak boson fusion signal process and for the QCD background processes, we generate events in which a Higgs boson is produced along with two jets that carry large transverse momentum. The effectiveness of different prescriptions to enhance the signal-to-background ratio is studied, and the expected signal purities are calculated in each case. We find that a simple cut on the rapidity of one final-state jet works well. We determine that an accuracy of $\delta g/g \sim 10\%$ on the effective coupling g may be possible after $\sim 200 \text{ fb}^{-1}$ of integrated luminosity is accumulated at the Large Hadron Collider.

DOI: 10.1103/PhysRevD.70.073011

PACS numbers: 14.80.Bn, 12.38.Bx, 12.38.Qk, 13.85.-t

I. INTRODUCTION

Following the discovery of the neutral Higgs boson H at the CERN Large Hadron Collider (LHC), attention will focus on the measurement of its couplings to gauge bosons and fermions. A promising reaction from which to extract some of these couplings, particularly the HWW coupling, is the weak boson fusion (WBF) process [1–14], where the Higgs boson H is produced via fusion of the weak bosons W and Z : $WW, ZZ \rightarrow H$, and is accompanied in the final-state by two jets that carry large transverse momentum p_T . To extract the couplings reliably, a good understanding is required of the production processes and the background processes that lead to the same final-state. Many strong interaction subprocesses also generate Higgs boson-plus-two-jet ($H + 2$ jet) final states. These background subprocesses can be computed with the techniques of perturbative quantum chromodynamics (QCD). They supply an *irreducible* background that may be reduced to some extent by judicious selections on the final-state event topology.

In the analysis presented here, we have in mind a situation in which the Higgs boson has been discovered and a sample of events exists containing a Higgs boson and two or more jets. This set of events will contain backgrounds of two types: real $H + 2$ jet events produced by QCD mechanisms other than WBF, and events which contain jets and particles that are present in typical Higgs boson decay modes, but without an explicit Higgs boson. Within the full event sample, we discuss the simulation of the real WBF signal and the irreducible QCD $H + 2$ jet background. We do not address the second type of contamination, such as events from the QCD $Z + 2$ jets process where the Z decay imitates a Higgs boson decay. Our concern is to estimate the expected signal purity, by

which we mean the fraction of real Higgs boson events produced by weak boson fusion.

The WBF $H + 2$ jet signal region is characterized by jets that carry large transverse momentum and large rapidity. Because the jets carry large transverse momentum, it is necessary to use hard QCD matrix elements in order to represent the signal and the $H + 2$ jet background reliably. A parton shower approach, for example, would be unlikely to provide a correct estimate of the momentum distribution of the jets in the region of phase-space of interest. Next-to-leading order (NLO) QCD corrections to the total WBF production cross section have been known for some time [15], and the corresponding corrections were calculated recently in a fully differential way [16]. In this paper, we use an independent calculation to verify the results of Ref. [16] and to examine in more detail the effects of the WBF selection cuts on the NLO QCD corrections. We also use perturbative QCD expressions for the background $H + 2$ jet matrix elements. At present, the fully differential $H + 2$ jet background distributions are known only at leading order. In addition to our NLO study of the signal process, we nevertheless provide two estimates of the NLO enhancement of the QCD $H + 2$ jet background process, in order to better assess the viability of the WBF channel for measuring the coupling strength of the Higgs boson to vector bosons. Our calculations are fully differential at the partonic level. One limitation of the fact that we omit showering is that forward beam jets, which likely have low p_T , are ignored.

Since the WBF channel is most interesting for a Higgs boson in the mass range $m_H = 115\text{--}200 \text{ GeV}$, we perform calculations with the two extremal values of this range. We compute differential cross sections in rapidity and transverse momentum at a pp collider with $\sqrt{s} = 14 \text{ TeV}$. In Sec. II, we discuss the production processes that contribute to the WBF signal and backgrounds, and we describe our method for evaluating them. We generate

*Electronic address: berger@anl.gov

†Electronic address: johnmc@hep.anl.gov

momentum distributions using the general purpose Monte Carlo program MCFM [17]. In our case, all jets carry a minimum value of relatively large transverse momentum whose values we specify.

We present numerical values of the differential cross sections in Sec. III. Various prescriptions are used in the literature to define the WBF sample, cuts that enhance the WBF fraction of the cross section by exploiting the special character of WBF events. Our investigations lead us to propose a new, somewhat simpler definition in terms of a cut on the rapidity of one of the final-state jets. In this section, we also define quantitatively what we mean by WBF signal purity P . We find that purities of 60% to 70% can be expected if a selection of $p_T \geq 40$ GeV is made on the tagging jets and somewhat lower values if the cut is dropped to 20 GeV. We derive an expression for the expected uncertainty on the effective Higgs boson-to-weak boson coupling strength g in terms of P , the expected statistical accuracy of LHC experiments, and the uncertainties on the signal and the background processes. We estimate that it should be possible to achieve an accuracy of $\delta g/g \sim 10\%$ after $\sim 200 \text{ fb}^{-1}$ of integrated luminosity is accumulated at the LHC. Somewhat smaller values of $\delta g/g$ are obtained in another recent investigation of anticipated uncertainties in the couplings [18], and we explain the source of the difference.

In Sec. IV, we compare the effects on both event rates and signal purity of our proposed method for defining WBF events with two other popular methods found in the literature: a selection on the difference in rapidities between two tagging jets in the final-state, and a selection on the invariant mass of a pair of tagging jets. The alternative prescriptions yield some increase in signal purity with respect to our definition, but the gain is sensitive to the cut in transverse momentum used to specify the trigger jets, and it is accompanied by loss of event rate. For values of the jet cut $p_T > 40$ GeV, our prescription appears to work about as well as the other methods. Relatively high-luminosity will be needed for a precise determination of the uncertainty $\delta g/g$. Our simpler definition of the WBF sample in terms of a selection on the rapidity of only one jet offers advantages in a high-luminosity environment where a large value of the transverse momentum cut is appropriate and multiple events per crossing may be an issue.

We provide two methods for estimating the size of next-to-leading order corrections to the $H + 2$ jet background in Sec. V. One of these relies on similarity with the $Z + 2$ jet process for which fully differential NLO results are known. The other method is an extrapolation from the known next-to-next-to-leading order (NNLO) results for the fully inclusive Higgs boson production process. The substantially different estimates for the NLO enhancement provided by these two methods show the level of uncertainty of the LO background calculation. A fully

differential NLO calculation of the $H + 2$ jet background applicable in the region of interest for WBF investigations is needed in order to improve our computations of signal purity and of the expected uncertainty in $\delta g/g$. A summary of our conclusions may be found in Sec. VI.

II. PRODUCTION CROSS SECTIONS

Examples of the WBF diagrams that must be calculated are shown in Fig. 1. The basic leading order process is shown in 1(a), where the exchanged bosons may be either W 's or Z 's, and one or both quark lines may be reversed, yielding qq , $q\bar{q}$ and $\bar{q}\bar{q}$ initial states. The virtual NLO corrections are obtained by adding a gluon loop to either qqV vertex, as illustrated in 1(b). The remaining real NLO corrections are shown in 1(c), where either an additional gluon is radiated in the final-state or a gluon from the proton splits into a $q\bar{q}$ pair. Calculation of the necessary loop diagrams is straightforward, providing a couple of simplifying assumptions are made. First, we ignore contributions of the form $q\bar{q}' \rightarrow V^* \rightarrow VH$, where $V = W, Z$. Second, we neglect any interference effects from identical flavor quarks in the final-state. We checked that both of these approximations have little effect on the calculated cross sections at leading order, particularly in the region of phase-space that we consider.

The NLO calculation is embedded in the general purpose Monte Carlo program MCFM [17], which uses the dipole subtraction method [19]. We use the default set of

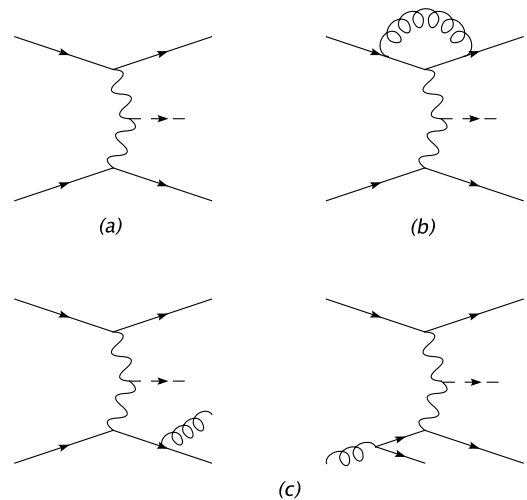


FIG. 1. Representative diagrams for the production of a Higgs boson via weak boson fusion: (a) at lowest order; (b),(c) at NLO. Further diagrams can be obtained by crossing incoming and outgoing lines in all cases. All of the virtual corrections are of the vertex correction form, as shown in (b). There are two types of real corrections depicted in (c). The first set corresponds to the emission of a gluon in all possible positions on the quark lines (left-hand diagram) and the second set corresponds to the crossing where a gluon is present in the initial-state (right-hand side).

parameters in this program, in which $\alpha = 1/128.89$, $M_W = 80.419$ GeV, $M_Z = 91.188$ GeV, and $\sin^2\theta_w = 0.2285$. For the parton distribution functions, we use CTEQ6L1 for lowest order and CTEQ6M at NLO [20]. In these sets of parton densities, $\alpha_s^{\text{LO}}(M_Z) = 0.130$ and $\alpha_s^{\text{NLO}}(M_Z) = 0.118$. In this paper, we choose the reference value $\mu = m_H$ for the renormalization and factorization scales. In Sec. III C we investigate the uncertainty of the signal and of the background associated with variation of the scale over the interval $2m_H > \mu > m_H/2$.

A. Generic cuts

The hallmark of WBF events is a Higgs boson accompanied by two ‘‘tagging’’ jets having large p_T and large rapidity. In real events and in computations at NLO, there are generally more than two jets, and the goal is to pick out a clean signal. To simplify our study and to demonstrate the robust character of the WBF process, it is desirable to make as few selections (cuts) as possible on the events. We begin with a basic set of cuts, exactly as in Ref. [16]. Jets obtained from the Monte Carlo runs are clustered according to the k_T algorithm with $p_T^{\text{jet}} > 20$ GeV, jet pseudorapidity $|\eta^{\text{jet}}| < 4.5$, and jet separation $\Delta R_{jj} = \sqrt{\Delta\eta_{jj}^2 + \Delta\phi_{jj}^2} > 0.8$, where $\Delta\phi_{jj}$ is the difference in the azimuthal angles of the two jets in the transverse plane. The two jets with the highest p_T are chosen as the tagging jets and ordered according to their pseudorapidities, $\eta_{j_1} < \eta_{j_2}$. In order to approximate the acceptance for the Higgs boson decay products and to complete the specification of our minimal set of cuts, we imagine the decay of a Higgs boson to two charged particles, denoted as ‘‘leptons’’. We require that these leptons satisfy the cuts:

$$p_T^{\text{lept}} > 20 \text{ GeV}, |\eta^{\text{lept}}| < 2.5, \Delta R_{j\ell} > 0.6, \eta_{j_1} < \eta_{\text{lept}} < \eta_{j_2}.$$

The Higgs boson decay products are therefore located in pseudorapidity between the two high- p_T jets. Although we enforce these cuts on potential Higgs boson decay products, the cross sections that we present do not include any branching ratio for this decay. We include branching ratios and efficiencies when we discuss the determination of the coupling strength in Sec. III.

Throughout this paper we refer to the QCD production of a Higgs boson in association with jets as the ‘‘background’’ to our WBF signal events. This cross section is implemented in MCFM at leading order based on the matrix elements of Ref. [21]. A selection of the contributing diagrams is shown in Fig. 2. There are contributions from qq , qg , and gg initial-state subprocesses, but the Higgs boson is always produced from an effective $gg \rightarrow H$ vertex. The effective coupling of the Higgs boson to two gluons is included in the limit of heavy top-quark mass m_t , with a coupling strength $\alpha_s/(3\pi v)$, where v is the Higgs boson vacuum expectation value, and α_s is

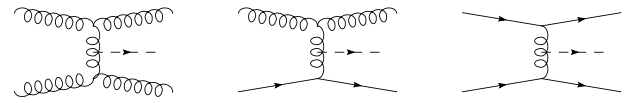


FIG. 2. Representative diagrams for the production of a Higgs boson and two jets at lowest order, calculated in the heavy top-quark limit of the Hgg effective coupling.

evaluated at the scale m_H with the 1-loop expression for the evolution (0.125 for $m_H = 115$ GeV and 0.116 for $m_H = 200$ GeV). The effective coupling approximation should be valid since we limit ourselves to Higgs boson masses $m_H < 2m_t$ and Higgs boson transverse momenta $p_T^H < m_t$ [22].

In Sec. V we estimate the NLO corrections to the lowest order result for the $H + 2$ jets background process by comparison with the similar $Z + 2$ jets process, calculated at NLO in Ref. [17,23], and by extrapolation from NNLO calculations of the fully inclusive process $pp \rightarrow HX$ [24–30], and NLO calculations of $pp \rightarrow H + 1\text{jet} + X$ [31].

III. RESULTS

The cuts mentioned in the previous section are a generic set of cuts. They do not exploit the kinematic structure of WBF events, where the jets tend to be produced very forward in pseudorapidity. In this subsection, we present first the cross sections for the signal and background processes after application of the generic cuts. Without further cuts, the WBF events would be lost in the QCD continuum background. We then apply one additional constraint which defines our WBF sample, and we show results for kinematic distributions, event rates, and signal purities.

A. Basic cuts

We examine the effects of the generic cuts in terms of their effects on the WBF signal and the $H + 2$ jet background. These cross sections—without any further cuts—are shown in Table I as a function of the minimum jet p_T . The WBF signal process is calculated at NLO and, at this point, the $H + 2$ jet background at LO. We remark

TABLE I. Cross sections in fb for the WBF signal (calculated at NLO) and $H + 2$ jet background (LO), as a function of the minimum jet p_T . Only the minimal set of cuts of Sec. II is applied.

p_T cut [GeV]	20	40	80
Signal ($m_H = 115$)	1866	1081	239
Bkg	2173	743	200
Signal ($m_H = 200$)	1189	709	166
Bkg	958	340	96

that the effects of the NLO corrections on the WBF process are rather small in this region, corresponding to K -factors between 0.95 and 1.1, depending on the Higgs boson mass and p_T cut.

The values in the table show that (without consideration yet of NLO effects in the background) the rates for the signal and background are comparable for $p_T^{\min} = 20$ GeV, and the signal-to-background ratio improves as the p_T cut is increased. The WBF signal lies above the $H + 2$ jet cross section if $p_T^{\min} \geq 40$ GeV.

B. WBF cuts

In an attempt to exploit the WBF event structure, a popular cut invokes a separation in pseudorapidity between the two tagging jets, for instance $|\eta_{j_1} - \eta_{j_2}| > 4$.

In this paper, we define a slightly different and simpler cut, motivated by our examination of the distributions of the absolute jet pseudorapidities shown in Fig. 3. In these figures, each tagging jet enters with weight one-half and cross sections have been converted to event rates with an integrated luminosity of 1 fb^{-1} . The area under each curve is equal to the total number of events in that channel.

The plots in Fig. 3 show that the shape of the distribution depends little on either the Higgs boson mass or the jet p_T , but—as expected—is very different in the signal process, compared to the $H + 2$ jet background. In each case, the WBF events peak at values of $|\eta| \approx 3$, although there is a slight movement to lower values of $|\eta|$ as the p_T cut is increased. The width of the peak also tends to decrease, but the full width at half-maximum is fairly

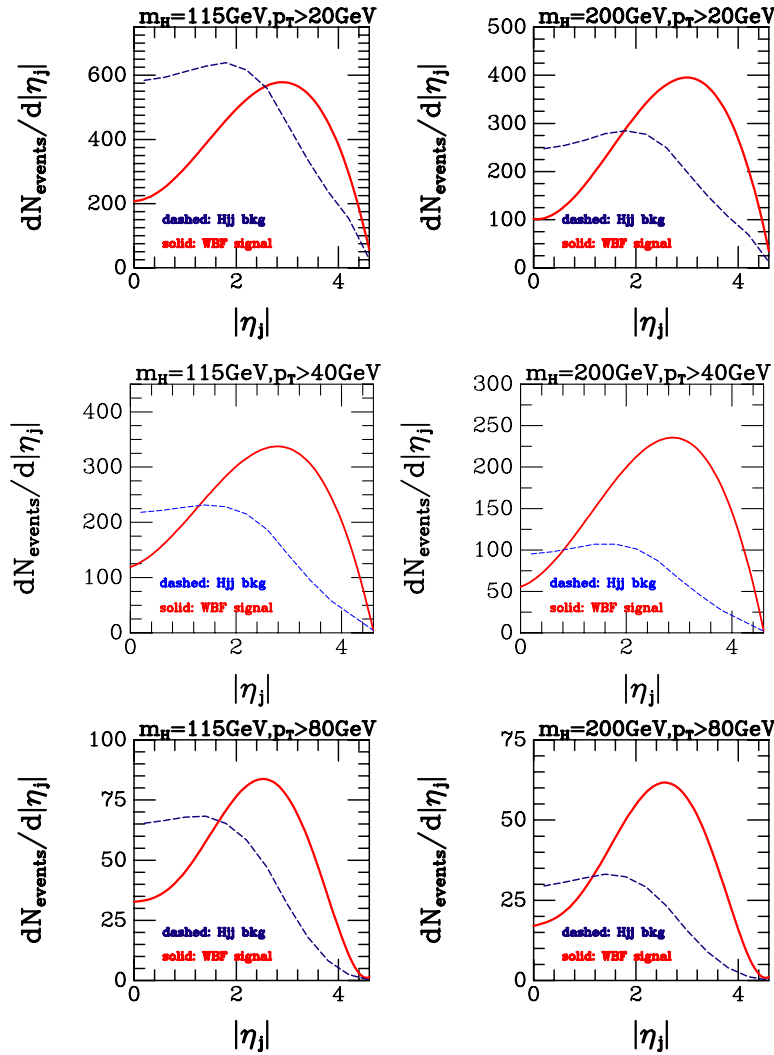


FIG. 3 (color online). Dependence of the tagging jet pseudorapidities on the minimum jet p_T used, for the two cases $m_H = 115$ GeV (left) and $m_H = 200$ GeV (right). Each of the two tagging jets in the event is entered in these plots, with weight one-half, and the rates assume an integrated luminosity of 1 fb^{-1} . The signal (solid line) is calculated at NLO and the background (dashed line) at LO. We show results for three different selections of the minimum jet transverse momentum, $p_T > 20, 40,$ and 80 GeV.

TABLE II. Event rates for the Hjj WBF signal (NLO) and Hjj background (LO), including our WBF requirement that at least one jet carry large $|\eta|$, as defined by Eq. (1). We assume 1 fb^{-1} of integrated luminosity. Purity is defined as $P = S/(S+B)$, where S stands for the number of signal events and B for the number of background events.

p_T cut [GeV]	20	40	80
Signal ($m_H = 115$)	1374	789	166
Bkg	1196	382	92
Purity	0.53	0.67	0.64
Signal ($m_H = 200$)	928	545	121
Bkg	534	179	46
Purity	0.63	0.75	0.72

constant at approximately three units of rapidity. In contrast, the rate of background events falls off fairly sharply beyond $|\eta| \approx 2$.

Motivated by the comparison of rapidity spectra in Fig. 3, and erring on the side of simplicity, we choose a uniform cut that ensures at least one jet lies within the peak. Namely,

$$\eta_{\text{peak}} - \eta_{\text{width}}/2 < |\eta_j| < \eta_{\text{peak}} + \eta_{\text{width}}/2, \quad (1)$$

for $j = j_1$ or $j = j_2$, where $\eta_{\text{peak}} = 3$ and $\eta_{\text{width}} = 2.8$.

Equation (1), along with the generic cuts specified above, constitutes our definition of weak boson fusion cuts. The effects of the pseudorapidity restriction on the jets are shown in Table II, where we have assumed 1 fb^{-1} of integrated luminosity. The rates in this table should be contrasted with those in Table I. In Table II, we include values for the signal purity, defined as $P = S/(S+B)$, where S stands for the number of signal events and B for the number of background events. The number of events as a function of the minimum jet p_T is also plotted in Fig. 4. Comparing the tables, one can see that the signal rate is diminished only slightly, by about 20%–30%. On

the other hand, the background is shrunk considerably, by about a factor of 2. A p_T cut of 20 GeV is barely sufficient to distinguish the WBF signal above the QCD LO Hjj background for $m_H = 115$ GeV. However, the signal S to background B ratio improves to about two for $p_T^{\text{cut}} \geq 40$ GeV. At $m_H = 200$ GeV, the situation is better, with S/B of about 1.7 when the p_T cut is 20 GeV, and rising to ~ 3 for $p_T^{\text{cut}} \geq 40$ GeV. A p_T cut of 40 GeV yields a prominent effect across the range of interesting masses, $m_H = 115$ –200 GeV.

It is instructive to examine the origin of the different rapidity spectra for the signal and the background. Since $H + 2$ jet events are generated in both cases with identical cuts on the transverse momenta of the jets, the different rapidity spectra must originate from dynamics. Comparing the LO production diagrams in Figs. 1 and 2, we note that gg and qg initial states contribute to the QCD background but not to the WBF signal. The gluon parton density is notably softer than the quark parton density, suggesting a plausible reason for the differences in the rapidity spectra of the final-state jets in the two cases. This reasoning is supported by the results shown in Fig. 5. The shape of the background rapidity spectrum from the qq , $q\bar{q}$, and $\bar{q}\bar{q}$ contributions is very similar to that of the signal, albeit with a slight shift of the peak to smaller $|\eta|$. The very different rapidity spectra of the signal and the background evident in Fig. 3 results therefore primarily from the gg and qg initial-state contributions. The results shown in Fig. 5 imply that there is a basic upper limit to the purity one can achieve for the WBF event sample, regardless of which prescription one adopts to define the WBF sample. The qq , $q\bar{q}$, plus $\bar{q}\bar{q}$ component of the QCD background process generates a final-state event topology essentially identical to the WBF signal process. Values of the purity are listed Table III; there is not much variation with m_H or the value of the cut in p_T . Our results suggest that purity is bounded from above by at most $P < 0.95$ at LHC energies.

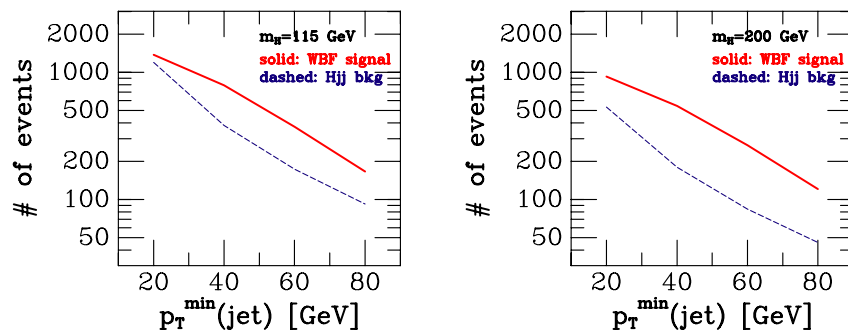


FIG. 4 (color online). Numbers of events for the WBF signal and the QCD background as a function of the minimum jet p_T , for an integrated luminosity of 1 fb^{-1} . No branching ratios for the Higgs boson decay have been applied. The pseudorapidity restriction on one of the jets has been enforced, as in Table II. The solid line is the NLO signal and the dashed line is the LO background.

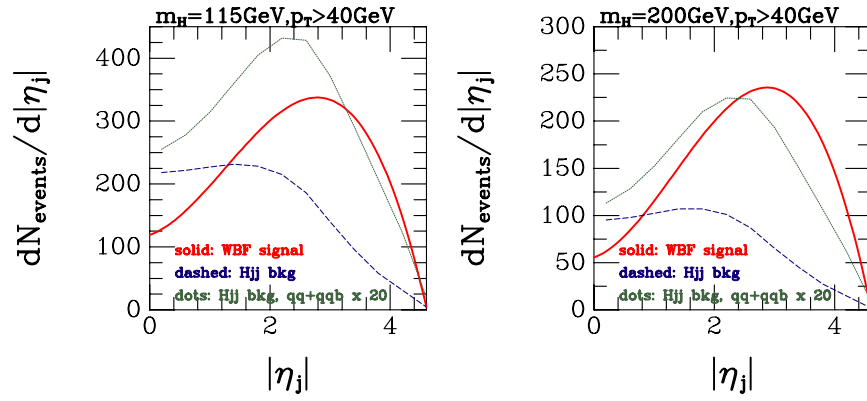


FIG. 5 (color online). Dependence of the tagging jet pseudorapidities for jet $p_T > 40$ GeV, for the two cases $m_H = 115$ GeV (left) and $m_H = 200$ GeV (right). For the background, we show the full result with all contributions included and, for comparison of shapes, the background obtained if only the qq , $q\bar{q}$, and $\bar{q}\bar{q}$ initial-state contributions are used. The magnitude of the separate component is multiplied by 20.

C. Scale dependence study

To examine further the effects of NLO corrections, we consider variation of the renormalization and factorization scale. A range of values $m_H/2 < \mu < 2m_H$ is used conventionally to estimate the theoretical uncertainty at a given order in perturbation theory. As a representative case, we show results for a minimum jet p_T of 40 GeV and both Higgs boson masses. In Fig. 6, we show the tagging jet pseudorapidity distributions for the signal and background for a range of values of the common renormalization and factorization scale μ . The signal process shows very little variation with μ , a shift of less than $\pm 2\%$ when $|\eta_j| \sim 2$ in the WBF signal region. In contrast, the $H + 2$ jet background at LO is enhanced by approximately 70% when the scale choice $\mu = m_H/2$ is made, and reduced by 40% for $\mu = 2m_H$. A fully differential NLO calculation of the $H + 2$ jet background process is required to reduce the large uncertainty associated with μ variation apparent in Fig. 6.

D. Uncertainty on the couplings

The signal and background events both include a real Higgs boson along with two jets. We may define a signal

TABLE III. Event rates for the Hjj WBF signal (NLO) and for the part of the Hjj background (LO) that arises from the qq , $q\bar{q}$, and $\bar{q}\bar{q}$ initial-state terms.

p_T cut [GeV]	20	40	80
Signal ($m_H = 115$)	1374	789	166
Bkg ($qq, q\bar{q}, \bar{q}\bar{q}$)	98	45	15
Purity ($qq, q\bar{q}, \bar{q}\bar{q}$)	0.93	0.95	0.92
Signal ($m_H = 200$)	928	545	121
Bkg	47	23	8
Purity	0.95	0.96	0.94

“purity” as the ratio $S/(S + B)$, where S denotes the number of signal events and B the number of background events. The purity as defined here does not improve with greater luminosity nor does it depend on the Higgs boson decay mode considered. Of interest to us is the effect of signal purity on the accuracy of the determination from data of the Higgs boson couplings g_{WW} and g_{ZZ} to the WW and ZZ channels. The WBF cross section is proportional to a combination of g_{WW}^2 and g_{ZZ}^2 , and their relative contribution changes somewhat with the value of the cut on p_T . In this paper, we discuss only an effective coupling strength g . We remark also that in our discussion of the expected accuracy on g , we limit ourselves to uncertainties at the level of production of the Higgs boson. We set aside uncertainties associated with the fact that the Higgs boson is observed only in specific final states and that all the final states cannot be observed above backgrounds.

To derive the uncertainty $\delta g/g$ on the coupling, we begin with the observed number of events $N = S + B$. We define the ratio $r = g_{\text{observed}}^2/g_{\text{predicted}}^2$. Then, under the assumption that any deviation in the expected total number of events arises from the effective coupling, we obtain $r = (N - B)/S$. Taking the total derivative, we obtain an expression for the uncertainty in r .

$$\delta r/r = \sqrt{\{(\delta S/S)^2 + [(\delta N)^2 + (\delta B)^2]/(N - B)^2\}}, \quad (2)$$

and, correspondingly,

$$\delta g/g = 1/2\sqrt{\{(\delta S/S)^2 + [(\delta N)^2 + (\delta B)^2]/(N - B)^2\}}. \quad (3)$$

With purity $P = S/(S + B)$, we derive

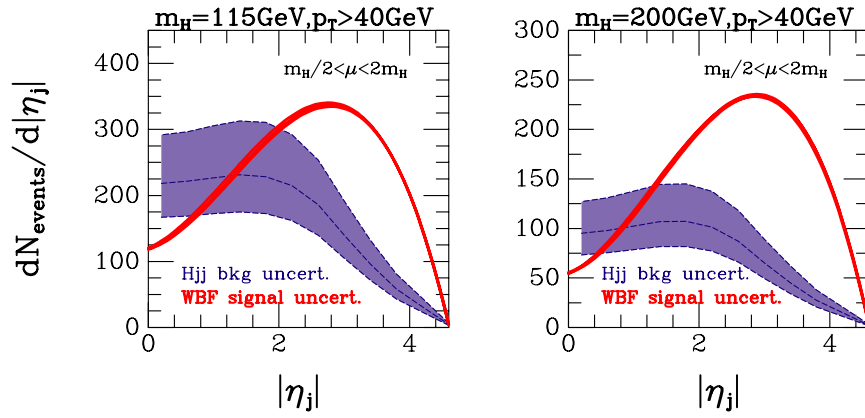


FIG. 6 (color online). Tagging jet pseudorapidity distributions in Hjj events, calculated with a range of values of the renormalization and factorization scale, μ . The signal (solid line) is calculated at NLO and the background (dashed line) at LO.

$$\delta g/g = 1/2\sqrt{\{(\delta S/S)^2 + (1/P)^2(\delta N/N)^2 + [(1-P)/P]^2(\delta B/B)^2\}}. \quad (4)$$

In the absence of any uncertainty in knowledge of the signal and background, Eq. (4) demonstrates the obvious fact that the best one can achieve is $\delta g/g = 0.5\delta N/N$ for $P = 1$. The factor $(1/P)$ that multiplies $\delta N/N$ in Eq. (4) shows that reduction in the purity effectively reduces the statistical power of the data. Similarly, the factor $(1-P)/P$ that multiplies $\delta B/B$ shows that greater purity diminishes the role of uncertainty in our knowledge of the background. Given that purity decreases as the background increases, we see that the size of the background in the WBF region is the problem to contend with; the uncertainty on the background is of less importance. To represent the background reliably in a region of phase-space in which tagging jets carry large transverse momentum, it is clearly important to use partonic hard matrix elements that can simulate this jet activity.

To obtain numerical values for the overall uncertainty in g , we must specify the uncertainties expected in our knowledge of the signal S and the background B , along with the statistical uncertainty $\delta N/N$. We address each of these contributions.

The NLO QCD effects on the WBF signal are modest as are uncertainties associated with parton densities and variation of the renormalization/factorization scale. We may take $\delta S/S = 5\%$, based on the calculated NLO μ dependence of $\pm 2\%$ and PDF uncertainty of $\sim 3\%$, both obtained in the WBF region of phase-space. Next-to-leading order QCD contributions to the background are discussed in Sec. V. The size of these contributions, scale dependence, and parton density variation could make the LO background estimate uncertain at the 60% level. We adopt a perhaps optimistic value of $\delta B/B = 30\%$. This choice presupposes that the 20% μ variation and 5% PDF uncertainty of the fully inclusive NLO cross section for

Higgs boson production may also apply to the NLO calculation of $H + 2$ jet production in the WBF region of phase-space, once this calculation is done.

Based on a study of conventional backgrounds [32], a minimum of roughly 10 fb^{-1} of integrated luminosity is needed to discover the Higgs boson in the WBF process. This figure would be achieved after 1-yr of LHC operation at a luminosity of $10^{33} \text{ cm}^{-2}\text{s}^{-1}$. Using the numbers in our Table II, we expect a WBF sample ($S + B$) of ~ 12000 events for $m_H = 115 \text{ GeV}$ and $p_{T\text{cut}} = 40 \text{ GeV}$, and ~ 7000 events for $m_H = 200 \text{ GeV}$ and $p_{T\text{cut}} = 40 \text{ GeV}$. To translate these event rates into statements about statistical significance, we must specify a Higgs boson decay mode and approximate tagging efficiencies for the decay products. For $m_H = 115 \text{ GeV}$, we choose the decay $H \rightarrow \tau^+\tau^-$, with one τ decaying leptonically and the other hadronically [8]. These choices yield a branching ratio of

$$\begin{aligned} Br(H \rightarrow \tau\tau) \times Br(\tau \rightarrow \text{leptons}) \times Br(\tau \rightarrow \text{hadrons}) \\ = 0.073 \times 0.7 \times 0.65 = 0.033. \end{aligned}$$

For the efficiency for tagging hadronic τ decays, we take the figure 0.26 from Ref. [33] as an optimistic upper bound.¹ The true value for this efficiency will be known only after analysis of data from LHC experiments. While our choice of tagging efficiency may seem large, it is relatively easy to scale our final results if a different value is preferred. The combination of branching fraction and efficiency results in a reduction in the number events by a factor $\epsilon = 0.033 \times 0.26 \approx 0.01$. For $m_H = 200 \text{ GeV}$, the

¹We recall that the generic acceptance cuts defined in Sec. II for the Higgs boson decay products are included in our event rates.

decay $H \rightarrow W^+W^-$ is prominent, and we select the case in which both W 's decay leptonically [11].² We obtain

$$\epsilon = Br(H \rightarrow WW) \times Br(W \rightarrow \text{leptons})^2 = 0.74 \times 0.22^2 = 0.036.$$

Using these numbers, we compute expected statistical uncertainties of $\delta N/N \sim 10\%$ and $\sim 6\%$ at $m_H = 115$ and 200 GeV, respectively. With statistical accuracy $\delta N/N$ of 10% , $\delta S/S = 5\%$ and $\delta B/B = 30\%$, we obtain $\delta g/g \simeq 10\%$ for purity $P = 0.7$ when $m_H = 115$ GeV, and $\delta g/g \simeq 8\%$ when $m_H = 200$ GeV.

After five years of LHC operation, we can anticipate an integrated luminosity of 200 fb^{-1} will have been accumulated. This increase allows us to reduce our estimates of $\delta N/N$ to $\sim 2\%$ and $\sim 1.5\%$ at $m_H = 115$ and 200 GeV, respectively, and $\delta g/g \sim 7\%$ for $P = 0.7$.

We remark that the uncertainties in the signal S and background B dominate the uncertainty in g . If $P = 0.7$ and $\delta N/N = 2\%$, then the uncertainties $\delta S/S$ and $\delta B/B$ would have to be reduced to 3% and 6% , respectively, before the statistical uncertainty would control the answer. Even if $P = 1$, $\delta g/g$ is controlled by $\delta S/S$ until $\delta S/S \leq \delta N/N$.

In Fig. 7, we show numerical predictions for the uncertainty as a function of purity, for two choices of the statistical uncertainty. Signal purities of 0.65 or greater permit determinations of $\delta g/g$ of 10% or better after 200 fb^{-1} have been accumulated. As shown in Table II, $P > 0.65$ is obtained for $p_{T\text{cut}} > 40$ GeV at $m_H = 115$ GeV, and $p_{T\text{cut}} > 20$ GeV at $m_H = 200$ GeV. The curves indicate to us that there is not much to gain from purities greater than 70% .

Somewhat smaller values of $\delta S/S$ and $\delta B/B$ are chosen in another recent investigation of anticipated uncertainties in the couplings [18]. These values are $\delta S/S = 4\%$ and $\delta B/B = 20\%$. Although the scope of that study is quite different from ours, we may compare our estimates with theirs. In Fig. 8, we show the uncertainty as a function of purity for these new estimates of $\delta S/S$ and $\delta B/B$. For $P = 0.7$, we now find $\delta g/g \sim 9\%$ and $\sim 5\%$ for the low- and high-luminosity data samples. This new lower value of $\delta g/g$ is similar to that obtained in Ref. [18] at comparable luminosity.³

²We acknowledge that $H \rightarrow W^+W^-$ with leptonic decay of both W 's is not a perfect match to our earlier specification of two body decay of the Higgs boson to leptons. Because the W is fairly massive, the rapidity distribution of the decay leptons may extend beyond $|\eta| < 2.5$, and a further acceptance correction may have to be applied. Such a study is best addressed by an experimental simulation of the entire decay chain.

³One must bear in mind that the uncertainty discussed in Ref. [18] is the uncertainty on g^2 and therefore a factor of 2 greater.

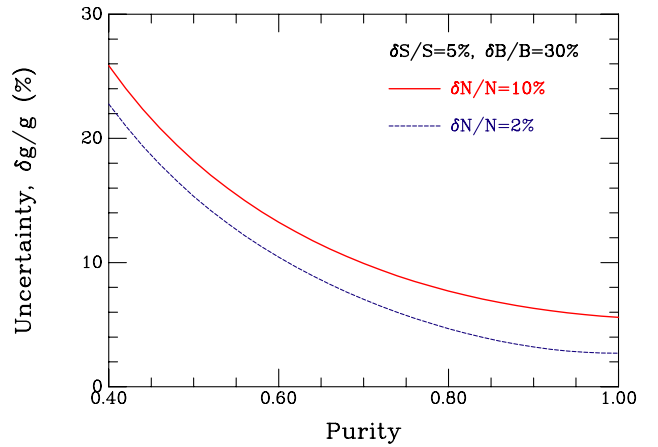


FIG. 7 (color online). The predicted uncertainty $\delta g/g$ in the coupling of the Higgs boson to a pair of W bosons is shown as a function of signal purity $P = S/(S + B)$ for expected statistical accuracies $\delta N/N$ of 10% and 2% . The uncertainties in knowledge of the signal S and background B are assumed to be 5% and 30% , respectively.

IV. ALTERNATIVE DEFINITIONS OF THE WBF SAMPLE

In the previous section, we define the WBF sample by a simple selection on the rapidity of one jet in an event in which there is a Higgs boson and two jets each carrying p_T greater than a specified minimum value. Other definitions have been used in the literature, and we wish to compare our signal rates and purities with those obtained if we use these alternatives. We examine the traditional cut on rapidity separation between the two trigger jets and a cut on the invariant mass of the pair of trigger jets.

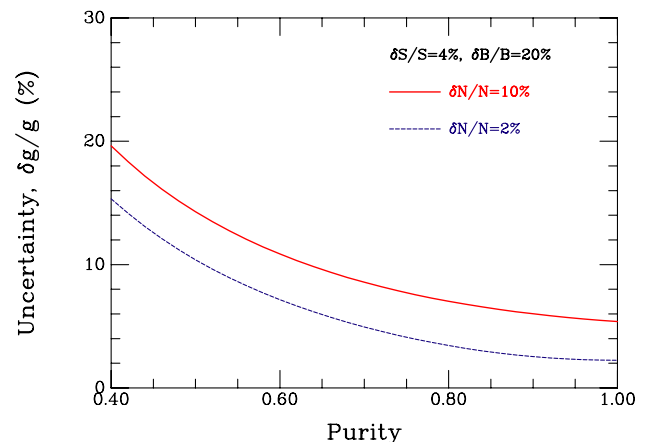


FIG. 8 (color online). The predicted uncertainty $\delta g/g$ in the coupling of the Higgs boson to a pair of W bosons is shown as a function of signal purity $P = S/(S + B)$ for expected statistical accuracies $\delta N/N$ of 10% and 2% . The uncertainties in knowledge of the signal S and background B are assumed to be 4% and 20% , respectively.

A. Rapidity separation cut

In Fig. 9, we illustrate the expected event rates as a function of the difference in rapidities between the forward and backward tagging jets. There is a clear separation in the locations of the peaks of the WBF signal and the background, not unlike that seen in our Fig. 3. Distributions such as these may motivate the choice of a cut on rapidity separation, $|\eta_{j_1} - \eta_{j_2}| > 4$, as in Refs. [1–14,16]. Signal and background rates for WBF events selected in this fashion are shown in Table IV. Comparison of Tables II and IV shows that the signal rate is diminished somewhat and that the purity is greater when the rapidity separation selection is made. As shown in Figs. 7 and 8, a gain in purity reduces the uncertainty in $\delta g/g$. The quantitative shift from $P = 0.67$ to $P = 0.78$ at $M = 115$ GeV and $p_T > 40$ GeV is an improvement of only 3% in $\delta g/g$, and this reduction is offset somewhat by the loss in statistical accuracy.

At lowest order in perturbation theory, one might expect naively that our simple rapidity selection and the rapidity separation cut are close to identical since there are only two jets in the event, tending to be located in opposite hemispheres. However, the finite rapidity carried by the Higgs boson introduces differences. Our preference for the simple rapidity cut is based on a few considerations. In data (and at yet-higher orders in perturbation theory), there will be many jets, and the simple specification of events that satisfy Eq. (1) will be easier to implement. Second, in a high-luminosity environment with more than one event per beam crossing, a selection on only one jet (in addition to the Higgs boson) reduces the chance that jets from different events are used. Finally, in our study of NLO event topologies with three jets in the final-state, we find that a gluon jet, rather than a quark jet is sometimes one of the two jets with largest p_T . For example, with a jet cut of 20 GeV and $m_H = 115$ GeV,

TABLE IV. Event rates for the Hjj WBF signal (NLO) and Hjj background (LO), without our WBF definition and instead with the rapidity separation cut $|\eta_{j_1} - \eta_{j_2}| > 4$. We assume 1 fb^{-1} of luminosity. The purity and significance are as defined before.

p_T cut [GeV]	20	40	80
Signal ($m_H = 115$)	1297	718	137
Bkg	758	207	38
Purity	0.63	0.78	0.78
Signal ($m_H = 200$)	911	521	106
Bkg	349	102	20
Purity	0.72	0.84	0.84

a gluon is a tagging jet about 25% of the time when we use our definition of WBF events.

B. Invariant mass cut

As an alternative to the rapidity separation cut, one might consider a cut on the invariant mass of the two trigger jets. In Fig. 10 and in Table V, we display the effects of the mass cut $M_{jj} > 800$ GeV. Comparison of Figs. 10 and 3 shows a decided improvement in the signal-to-background ratio, an effect that is borne out in the purity numbers shown in Tables V and II. However, the significant gain in purity is true only for the smaller values of the p_T cut and is accompanied by a substantial loss of signal rate. Since the smallest value of the p_T could be employed only with low-luminosity data samples, it is not evident that the price in loss of signal rate is affordable. The combination of the mass cut and our simple forward jet cut improves purity only slightly and reduces the signal rate further.

Using the invariant mass cut to define the WBF sample, we note that the number of events at $m_H = 115$ GeV with a cut on p_T of 20 GeV is very similar to what we obtain

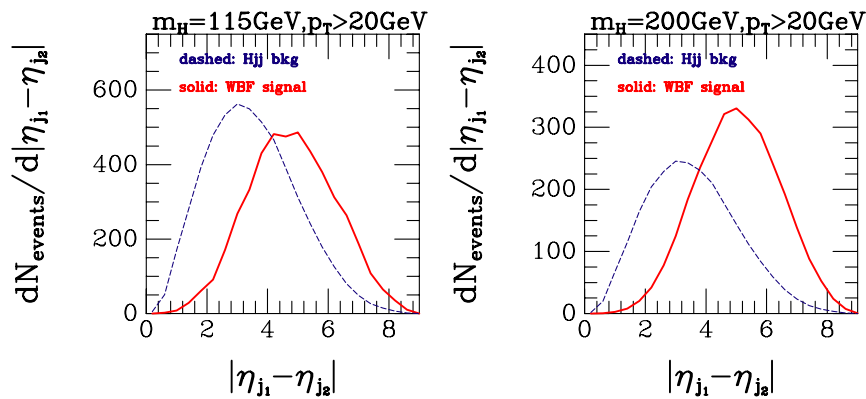


FIG. 9 (color online). The difference between the two tagging jet pseudorapidities for a minimum jet p_T of 20 GeV, for the two cases $m_H = 115$ GeV (left) and $m_H = 200$ GeV (right). The rates assume an integrated luminosity of 1 fb^{-1} . The signal (solid line) is calculated at NLO and the background (dashed line) at LO.

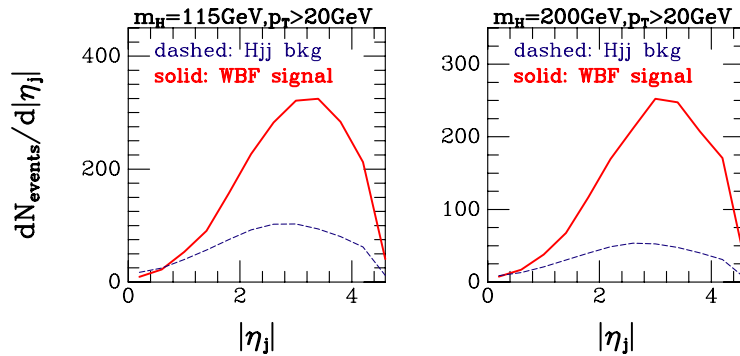


FIG. 10 (color online). The tagging jet pseudorapidity distribution for a minimum jet p_T of 20 GeV, for the two cases $m_H = 115$ GeV (left) and $m_H = 200$ GeV (right)—with a minimum dijet invariant mass, $M_{jj} > 800$ GeV. Each of the two tagging jets in the event is entered in these plots, with weight one-half, and the rates assume an integrated luminosity of 1 fb^{-1} . The signal (solid line) is calculated at NLO and the background (dashed line) at LO.

with our WBF prescription but with a cut on $p_T = 40$ GeV. The purities are also nearly the same. This comparison would seem to favor our simple prescription: a larger value of the cut on p_T is more appropriate in a high rate environment and more effective at reducing backgrounds not considered here. We conclude this section with the remark that the alternative prescriptions of the WBF sample in terms of either a rapidity separation cut or an invariant mass cut yield some increase in the signal purity with respect to our simple cut on the rapidity of one jet, but the gain depends on the value of the cut on p_T of the jets and is accompanied by some loss of event rate. As long as hard matrix elements are used to generate the p_T distributions of the jets, all three methods yield similar event samples. On the other hand, significant differences seem to result if one uses a parton shower method to generate the $H + 2$ jet background [32]. In our view, the hard matrix element approach is a more faithful representation of the momentum distributions of jets in the relevant WBF region of large p_T .

V. ESTIMATES OF THE Hjj NLO CORRECTIONS

A differential calculation of the Hjj background does not exist at next-to-leading order. Prior to undertaking

TABLE V. Event rates for the Hjj WBF signal (NLO) and Hjj background (LO), without our usual WBF definition and instead with $M_{jj} > 800$ GeV. We assume 1 fb^{-1} of luminosity.

p_T cut [GeV]	20	40	80
Signal ($m_H = 115$)	808	561	158
Bkg	304	183	82
Purity	0.73	0.75	0.66
Signal ($m_H = 200$)	617	428	121
Bkg	157	95	43
Purity	0.80	0.82	0.74

such an effort, we wish to obtain plausible estimates of the sizes of NLO effects on both event rates and kinematic distributions. We present two such estimates in this section.

The NLO corrections for QCD production of a Z boson in association with two jets are known [17,23]. Representative diagrams for this process—seen in Fig. 11—can be compared with those for H plus two jets, shown in Fig. 2. Our first estimate of NLO effects for Hjj is based on its similarity with Zjj , but we acknowledge some important differences. In the Hjj process the Higgs boson couples only to gluons (via a top-quark loop), whereas the Z boson couples only to quarks. This difference means that the processes have a different sensitivity to the parton distribution functions. Second, the couplings of the scalar Higgs boson to the decay products are also different, and the angular distributions of the decay products differ in the two cases. While we do not include a decay branching ratio, our cuts require the rapidities of decay products of the produced boson to lie between those of the two tagging jets. Finally, the effective Hgg coupling contains a factor of α_s so that the Hjj process is formally proportional to α_s^4 , in contrast with α_s^2 for Zjj . Although the Hjj process is naively of $\mathcal{O}(\alpha_s^4)$, our use an effective coupling for the Hgg vertex means that the Hjj process is effectively of the same order, $\mathcal{O}(\alpha_s^2)$, as the Zjj process. Since we are interested only in Higgs boson masses that satisfy $m_H < 2m_t$, with transverse momenta $p_T^H < m_t$, the effective coupling approach is valid [22].

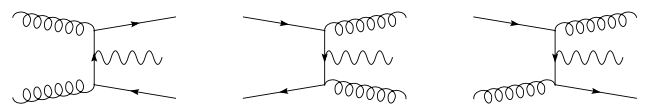


FIG. 11. Representative diagrams for leading order $Z + 2$ jet production.

We calculate the Zjj cross section using a variable Z -mass, $m_Z = m_H$. In this way, we estimate the NLO corrections for a process involving the QCD production of a heavy vector boson and two jets. We examine the distribution of the tagging jet pseudorapidities, as before. In particular, we are interested in whether the shape of this distribution changes significantly at NLO. A NLO effect that would modify the background distribution so that it resembles the signal peak, could have a serious effect on the ability to select the genuine WBF events.

We show the lowest order distributions for the Hjj and Zjj processes in Fig. 12. We do not reproduce the plots for more than one value of the p_T cut, since this cut does not alter the conclusions. One can see that the distributions for the two processes are very similar in shape in the two cases, differing in the behavior at low pseudorapidities—where the Zjj curve is somewhat higher—and toward the tail, where the Hjj distribution dies off slightly more slowly. For the purposes of this study, the most prominent difference—that at low values of $|\eta_j|$ —has little effect since our cuts require that $|\eta_j| > 1.6$ for at least one of the tagging jets. The remaining difference in shapes is small, and we conclude that, as a first estimate, our use of the Zjj process to approximate Hjj is reasonable.

For the Zjj process, the lowest order and NLO distributions in the tagging jet pseudorapidity are shown in Fig. 13. These are to be compared with the Hjj curves in Fig. 3. We show curves for two different boson masses, as before, and for a variety of p_T cuts. The NLO corrections do not appear to alter the shape of this distribution significantly. Moreover, with the scale choice $\mu = m_H$, the corrections are small in magnitude, both in the total cross section and over the pseudorapidity range of interest. The change in cross section is shown quantitatively in Table VI, where we show the K -factors for this process having applied all the WBF cuts. The corrections vary from $\approx 10\%$ for $m_Z = 200$ GeV and moderate $p_T = 20, 40$ GeV to $\approx -15\%$ for $m_Z = 115$ GeV and high $p_T = 80$ GeV.

In the definition of the K -factor in this paper, different parton distribution functions (PDF's) are used in the numerator and denominator, LO expressions in the denominator and NLO expressions in the numerator. Correspondingly, different values of α_s are used in the numerator and denominator:

$$K = \frac{\sigma^{\text{NLO}}[\text{CTEQ6M}; \alpha_s^{\text{NLO}}(\mu)]}{\sigma^{\text{LO}}[\text{CTEQ6L1}; \alpha_s^{\text{LO}}(\mu)]} \quad (5)$$

That the K -factors are close to unity for the Zjj process results from a compensation between the change in PDF from LO to NLO and the change in $\alpha_s(\mu)$, plus the effects of the additional processes at NLO. In $\alpha_s(\mu)$, the net change, after reduction in the value of $\alpha_s(M_Z)$ and the altered evolution, tends to decrease the cross section from LO to NLO, by a factor

$$\left[\frac{\alpha_s^{\text{NLO}}(\mu)}{\alpha_s^{\text{LO}}(\mu)} \right]^2 = 0.83,$$

for both cases ($\mu = 115, 200$ GeV). One must be careful to apply this K -factor consistently only to a lowest order calculation with the same PDF set and treatment of α_s . Since we use CTEQ6L1 in the background calculation of Table II, it is straightforward to incorporate these K -factors in order to obtain the new background estimates in Table VII, for an assumed 1 fb^{-1} of integrated luminosity. For the estimate of NLO corrections to the background presented in this section, with $\mu = m_H$, the table shows that the purity starts at about 50% at $m_H = 115$ GeV, if the cut on p_T is 20 GeV, and grows to about 70% when the p_T cut is 40 GeV or larger. Slightly larger values are obtained at $m_H = 200$ GeV.

We show in Fig. 14 the effect of a lower scale choice $\mu = m_H/2$ on the Zjj process. In contrast to Fig. 13, the NLO corrections are now substantial, negative, and not constant as the pseudorapidity changes. For this lower scale choice, we now apply the K -factors point-by-point to the lowest order Hjj background distribution in order

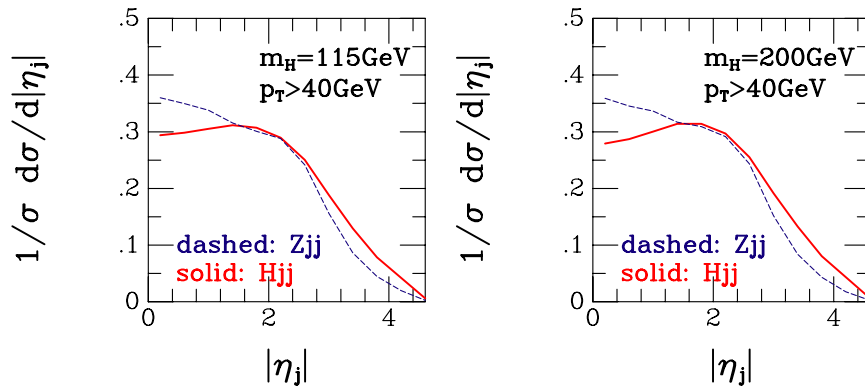


FIG. 12 (color online). Normalized LO tagging jet pseudorapidity distributions in Hjj (solid line) and Zjj (dashed line) events. The minimum jet p_T cut is 40 GeV; $m_H = 115$ GeV (left) and $m_H = 200$ GeV (right). For the Zjj events, the Z mass has been altered to $m_Z = m_H$.

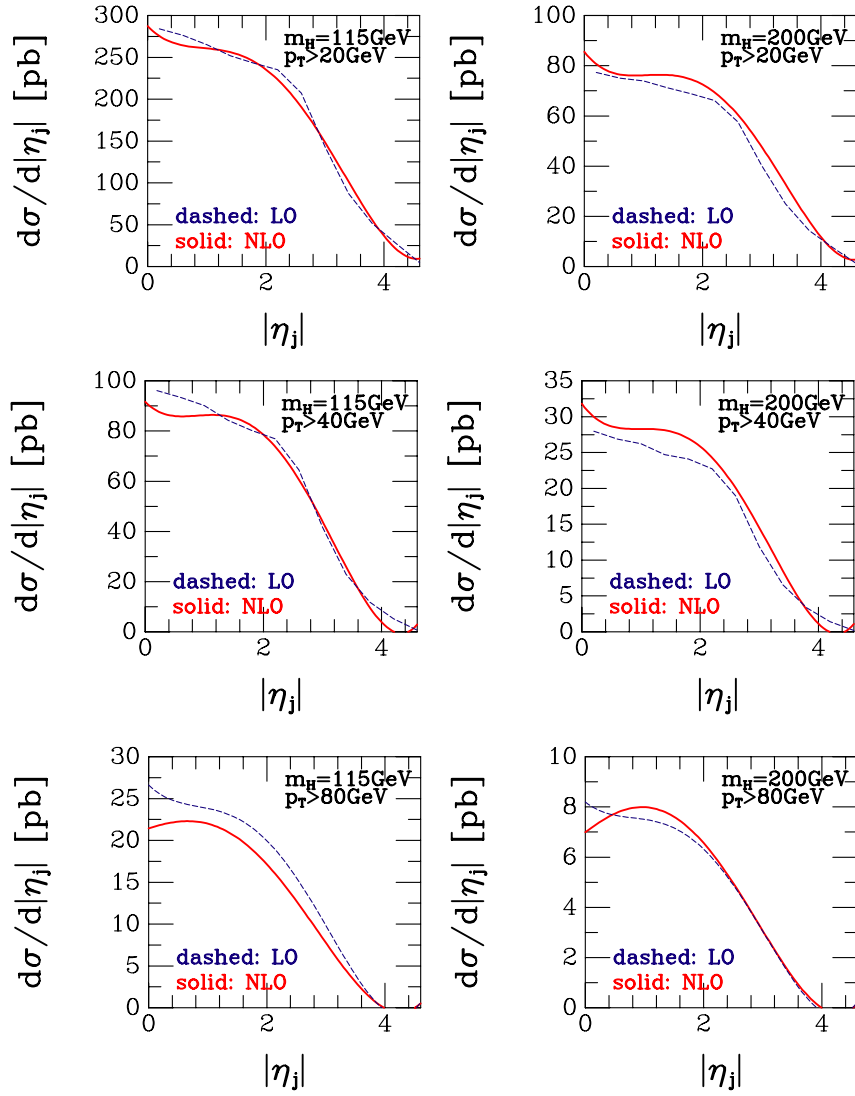


FIG. 13 (color online). Dependence of the tagging jet pseudorapidity in Zjj events on the minimum jet p_T cut, for the two cases $m_Z = 115$ GeV (left) and $m_Z = 200$ GeV (right). In each graph, the LO (dashed line) and NLO (solid line) curve is shown. The scale choice is $\mu = m_H$.

to estimate the new NLO result. The result of this exercise is shown in Fig. 15, along with the estimated NLO result for $\mu = m_H$. This figure shows that our estimate for the NLO Hjj background cross section is affected very little if we choose a smaller scale such as $\mu = m_H/2$. Reducing the scale, we find that the LO background is increased

TABLE VI. The K -factors, as defined by Eq. (5), for Zjj production with our WBF cuts. The Z mass has been altered to take on the two relevant Higgs boson mass values, $m_Z = m_H$, and the scale choice is $\mu = m_H$.

p_T cut [GeV]	20	40	80
$m_H = 115$	1.00	0.99	0.84
$m_H = 200$	1.12	1.11	1.02

substantially. However, the K -factor decreases in such a way as to restore the size of background at NLO.

TABLE VII. Event rates for the Hjj WBF signal (NLO) and Hjj background (estimated NLO), for an assumed 1 fb^{-1} of luminosity. No branching ratio is included for the Higgs boson decay.

p_T cut [GeV]	20	40	80
Signal ($m_H = 115$)	1374	789	166
Bkg	1196	378	77
Purity	0.53	0.68	0.68
Signal ($m_H = 200$)	928	545	121
Bkg	598	199	47
Purity	0.61	0.73	0.72

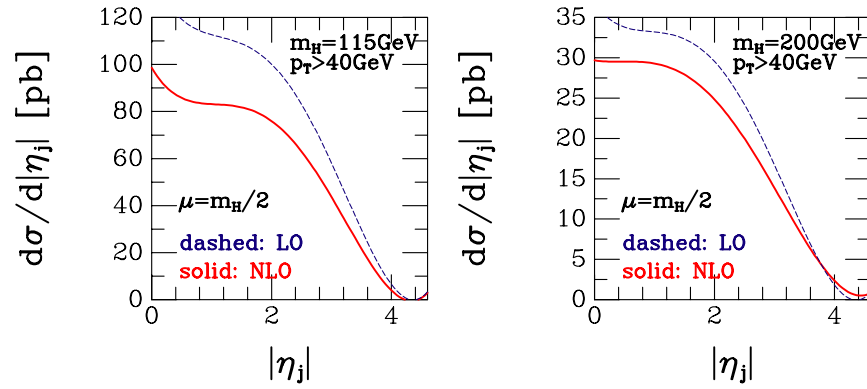


FIG. 14 (color online). Tagging jet pseudorapidity distributions in Zjj events, calculated with a smaller renormalization and factorization scale, $\mu = m_H/2$. In each graph, the LO (dashed line) and NLO (solid line) curve is shown.

A. Background estimate with a mass cut

In a similar spirit to the above study, here we present the estimate of the NLO corrections to the Hjj background when the definition of the WBF event sample involves only an invariant mass cut on the two tagging jets, $M_{jj} > 800$ GeV. In Fig. 16, we show the lowest order distribution of the invariant mass of the two tagging jets, for the processes Hjj and Zjj and a jet p_T cut of 40 GeV. Each curve is normalized by its own integrated cross section. Although the two distributions differ in shape considerably over such a wide range of M_{jj} , the two curves show similar behavior above $M_{jj} > 800$ GeV. We conclude again that the Zjj process will yield a reasonable estimate of the Hjj process in the region of phase-space of interest for WBF studies.

The effects of the NLO corrections for the Zjj process are shown in Fig. 17. They are small over the entire mass range, and they do not change the shape of the distribution. The net effect is summarized in Table VIII, where we show the K -factors for each p_T cut and Higgs mass for the alternative definition of the WBF sample, $M_{jj} > 800$ GeV. The corrections are universally negative, rang-

ing from $\approx -10\%$ for $m_Z = 200$ GeV to $\approx -20\%$ for $m_Z = 115$ GeV and the higher p_T cuts of 40, 80 GeV.

Using these K -factors, we can update the earlier leading order results of Table V. Since the K -factors are close to unity, the effect of the NLO corrections is small, as illustrated in Table IX. With NLO effects included, we conclude as at LO, that the cut on the jet-pair invariant mass improves the signal purity significantly with respect to our simple rapidity prescription only for the smallest of the cuts on p_T (*c.f.* results Table VII), but at a cost in the signal rate at all p_T .

B. Second estimate of NLO corrections to the background

A different and larger estimate of the NLO corrections to the Hjj background may be obtained if we begin with results for inclusive Higgs boson production processes. Corrections to the fully inclusive cross section are known both to NNLO [24–28] and with all-orders soft-gluon resummation included [29,30]. In addition, the NLO corrections to the $H + j$ process are published [31]. By starting from the inclusive process or the $H + j$ process,

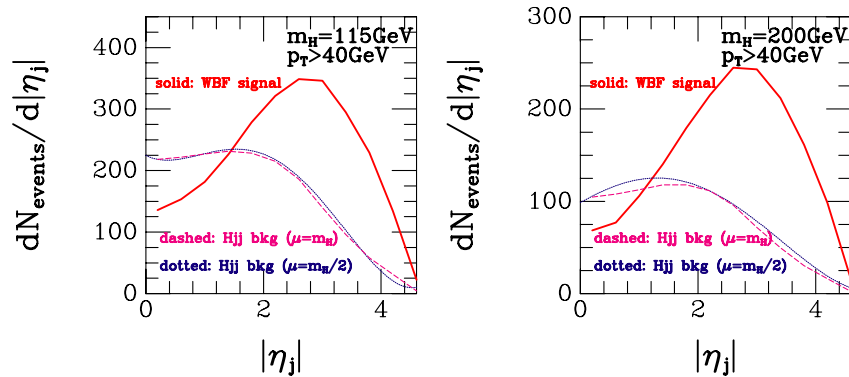


FIG. 15 (color online). Estimated tagging jet pseudorapidity distributions in Hjj events at NLO, calculated with a smaller renormalization and factorization scale, $\mu = m_H/2$. Also shown (lower curve) is the estimated NLO Hjj result with $\mu = m_H$.

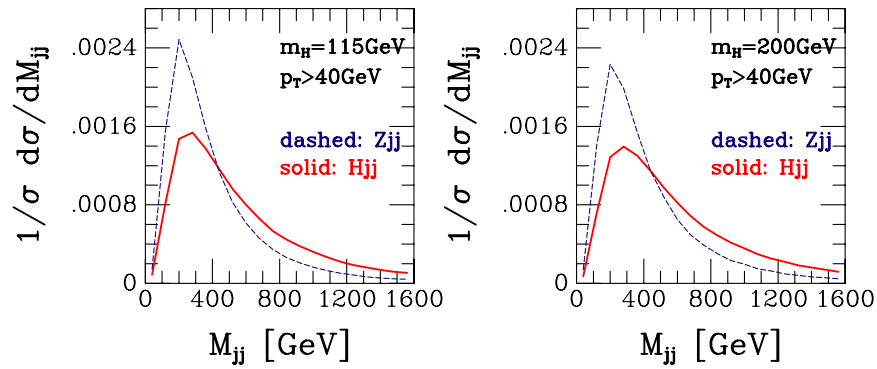


FIG. 16 (color online). Normalized LO tagging jet invariant mass distributions in Hjj (solid line) and Zjj (dashed line) events. The minimum jet p_T cut is 40 GeV; $m_H = 115$ GeV (left) and $m_H = 200$ GeV (right). For the Zjj events, the Z mass has been altered to $m_Z = m_H$.

we begin with a process that is dominated by gg scattering, unlike the Zjj case.

With the same definition of the K -factor used in this paper, and the same choice of renormalization/factorization scale, the result for the fully inclusive Higgs boson cross section is

$$K(H + X) = 1.7 - 1.8.$$

The increase at NLO is slightly larger at $m_H = 200$ GeV than at $m_H = 115$ GeV. For the semi-inclusive $H + j$ process, where an additional jet of $p_T > 20$ –80 GeV is specified in the final-state, the NLO corrections correspond to,

$$K(H + j + X) \approx 1.3 - 1.5.$$

In this case the PDF sets used were similar but not identical (CTEQ4), and this result is quoted for $m_H = 120$ GeV.

We now try to apply these K factors, obtained in situations in which either no jet or at most one jet is required in the final-state, to the case of interest here where two jets are required, each with a minimum value

of p_T , and with the other WBF cuts. In the case of $Z +$ jets, the K -factors are 1.14, 1.16, and 0.90 for 0, 1, and 2 jets, respectively [23], with the same PDF's and definition of K -factors used here. In other words, the K -factor is approximately independent of the number of specified jets. In Table VI, K -factors are shown for the Zjj process with WBF cuts applied. They are close to unity. In Ref. [23], the K -factor is obtained for the $Z + 2$ jet process with a jet cut of $p_T > 20$ GeV, but without the WBF cuts. It is also close to unity, $K = 0.9$. This value is similar enough to the numbers shown in Table VI to justify the assumption that the overall inclusive K -factor is not very different from the one that should be applied for WBF events. Adopting this line of argument, we suggest that a conservative estimate of the K -factor for Hjj production in the WBF region is a K -factor from the more inclusive processes above,

$$K(H + jj + X) \approx \frac{K(H + X) + K(H + j + X)}{2} = 1.6.$$

The new estimates of NLO corrections to the background are presented in Table X. The signal purity starts at about

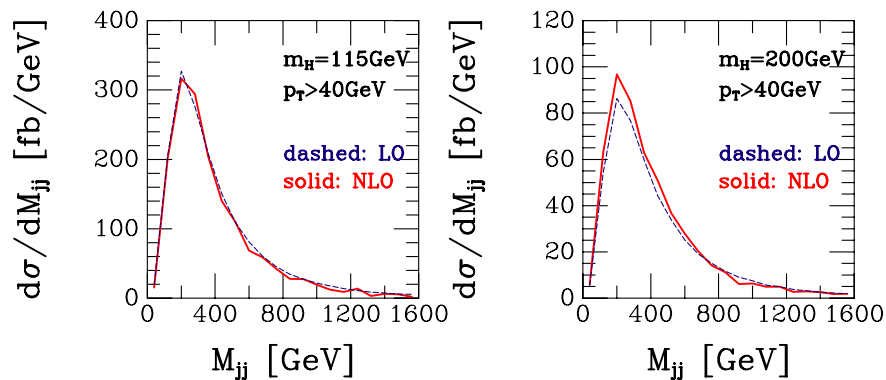


FIG. 17 (color online). Tagging jet invariant mass distribution in Zjj events with a jet p_T cut of 40 GeV, for the two cases $m_Z = 115$ GeV (left) and $m_Z = 200$ GeV (right). The LO (dashed line) and NLO (solid line) curves are shown, for a scale choice of $\mu = m_H$.

TABLE VIII. The K -factors, as defined by Eq. (5), for Zjj production with an alternative definition of the WBF cuts, $M_{jj} > 800$ GeV. The Z mass has been altered to take on the two relevant Higgs boson mass values, $m_Z = m_H$.

p_T cut [GeV]	20	40	80
$m_H = 115$	0.89	0.80	0.78
$m_H = 200$	0.93	0.93	0.89

40% when $m_H = 115$ GeV, if the cut on p_T is 20 GeV, and grows to about 60% when the p_T cut is 40 GeV or larger. Slightly larger values are obtained at $m_H = 200$ GeV.

With the larger background estimate of this subsection, the signal purity is lower than before (*c.f.* Table X vs Table VII). If the NLO enhancement of the background is as great as a factor 1.6, the value of $P \sim 0.4$ presented in Table X suggests that investigations with a low p_T cut will be ineffective. According to the results in Fig. 7, the uncertainty in $\delta g/g$ is quite large when $P < 0.5$. With the cut $p_T \geq 40$ GeV, the corresponding purities of $P \sim 0.6$ may still permit determinations of $\delta g/g \sim 10\%$. A fully differential NLO calculation of the background process for $H + 2$ jets is definitely needed to establish both the size of the background and the theoretical uncertainty $\delta B/B$.

VI. SUMMARY AND CONCLUSIONS

In this paper, we investigate the weak boson fusion process for production of the neutral Higgs boson H at the LHC. We are interested in estimating the accuracy with which the Higgs boson coupling to-weak bosons may be determined from data. An important and, in fact, controlling aspect is the extent to which events produced by the WBF subprocess may be separated from events in which a Higgs boson is produced by other mechanisms. A hallmark of the WBF subprocess is that the Higgs boson is accompanied in the final-state by two jets that carry large transverse momentum p_T and relatively large rapidity. However, purely strong interactions subprocesses also produce Higgs bosons accompanied by

TABLE IX. Event rates for the Hjj WBF signal (NLO) and Hjj background (estimated NLO), without our usual WBF definition and instead with $M_{jj} > 800$ GeV. We have assumed 1 fb^{-1} of integrated luminosity.

p_T cut [GeV]	20	40	80
Signal ($m_H = 115$)	808	561	158
Bkg	271	146	64
Purity	0.75	0.79	0.71
Signal ($m_H = 200$)	617	428	121
Bkg	146	88	38
Purity	0.81	0.83	0.76

two jets. To extract the couplings reliably, a good understanding is required of both the production and the background processes. We use hard QCD matrix elements in order to represent the signal and the $H + 2$ jet background reliably. We provide an independent calculation that verifies the fully differential next-to-leading order QCD corrections to the WBF signal process of Ref. [16], and we examine in more detail the effects of the WBF selection cuts on these NLO QCD corrections. We use leading order perturbative QCD expressions for the background $H + 2$ jet matrix elements since NLO results are not yet available in fully differential form. We also provide two estimates of the NLO enhancement of the QCD $H + 2$ jet background process. Our calculations are fully differential at the partonic level.

Among our goals in this study are to evaluate the effectiveness of different prescriptions for defining the WBF sample and to estimate the expected WBF signal purity P , by which we mean the fraction of real Higgs boson events produced by weak boson fusion.

Various prescriptions are used in the literature to define the WBF sample, cuts that enhance the WBF fraction of the cross section by exploiting the special transverse momentum and rapidity characteristics of WBF events. Our investigations lead us to propose a new, somewhat simpler definition in terms of a *cut on the rapidity of one of the final-state jets*, as defined by Eq. (1). We compare the effects on both event rates and signal-to-background ratio of our proposed method for defining WBF events with two other popular methods found in the literature: a selection on the difference in rapidities between two tagging jets in the final-state, and a selection on the invariant mass of a pair of tagging jets. In a low-luminosity environment where one may be tempted to use a relatively low cut on transverse momentum to select the trigger jets, the conventional alternatives provide better signal purity but at a cost in signal rate. Once the cut is raised, our definition does essentially as well in signal purity while preserving more of the signal.

We find that purities of 60% to 70% can be expected if a selection of $p_T \geq 40$ GeV is made on the tagging jets. We

TABLE X. Event rates for the Hjj WBF signal (NLO) and Hjj background (estimated NLO, according to the procedure in Sec. V B), for an assumed 1 fb^{-1} of integrated luminosity.

p_T cut [GeV]	20	40	80
Signal ($m_H = 115$)	1374	789	166
Bkg	1914	611	123
Purity	0.42	0.56	0.57
Signal ($m_H = 200$)	928	545	121
Bkg	854	286	74
Purity	0.52	0.67	0.62

derive an expression for the expected uncertainty on the effective Higgs boson-to-weak boson coupling strength g in terms of P , the expected statistical accuracy of the LHC experiments, and the theoretical uncertainties on the signal and the background processes. We estimate that an accuracy of $\delta g/g \sim 10\%$ may be achievable after $\sim 200 \text{ fb}^{-1}$ of integrated luminosity is accumulated at the LHC. On a cautionary note, however, we recall that our WBF signal purity and our uncertainties are obtained in a very well controlled situation in which there is an identified Higgs boson in a sample of $H + 2$ jet events produced by both the WBF mechanism and the QCD background processes. In an experimental context, there will be additional sources of background from final states that mimic a Higgs boson. The effects of these additional backgrounds presumably only increase the expected uncertainties on the couplings.

The theoretical uncertainties on the signal S , and on both the size and uncertainty of the background B dominate the uncertainty in g . Current estimates of $\delta S/S$ are

in the 5% range, and, since differential NLO calculations exist, this uncertainty is controlled by uncertainties in the parton densities and by the residual renormalization and factorization scale dependence. In order to reduce the estimated uncertainty in g , the next major step would appear to be a fully differential NLO calculation of the background applicable in the region of interest for WBF investigations.

ACKNOWLEDGMENTS

We thank T. LeCompte for valuable discussions and R. K. Ellis for collaboration in the early stages of this work. The authors gratefully acknowledge the Kavli Institute for Theoretical Physics, Santa Barbara for hospitality and support during the completion of the manuscript. This work was supported by the U. S. Department of Energy under Contract No. W-31-109-ENG-38 and in part by the National Science Foundation under Grant No. PHY99-07949.

-
- [1] R. Kinnunen and D. Denegri, hep-ph/9907291.
 - [2] V. Drollinger, T. Muller, and D. Denegri, hep-ph/0111312.
 - [3] E. Richter-Was and M. Sapinski, Acta Phys. Pol. B **30**, 1001 (1999).
 - [4] B. P. Kersevan and E. Richter-Was, Eur. Phys. J. C **25**, 379 (2002).
 - [5] D. Zeppenfeld, R. Kinnunen, A. Nikitenko, and E. Richter-Was, Phys. Rev. D **62**, 013009 (2000).
 - [6] D. Zeppenfeld, hep-ph/0203123.
 - [7] A. Belyaev and L. Reina, J. High Energy Phys. 08 (2002) 041.
 - [8] D. Rainwater, D. Zeppenfeld, and K. Hagiwara, Phys. Rev. D **59**, 014037 (1999).
 - [9] T. Plehn, D. Rainwater, and D. Zeppenfeld, Phys. Rev. D **61**, 093005 (2000).
 - [10] D. Rainwater and D. Zeppenfeld, Phys. Rev. D **60**, 113004 (1999); **61**, 099901(E) (2000).
 - [11] N. Kauer, T. Plehn, D. Rainwater, and D. Zeppenfeld, Phys. Lett. B **503**, 113 (2001).
 - [12] D. Rainwater and D. Zeppenfeld, J. High Energy Phys. 12 (1997) 005.
 - [13] O. J. Eboli and D. Zeppenfeld, Phys. Lett. B **495**, 147 (2000).
 - [14] D. Cavalli *et al.*, hep-ph/0203056.
 - [15] T. Han, G. Valencia, and S. Willenbrock, Phys. Rev. Lett. **69**, 3274 (1992).
 - [16] T. Figy, C. Oleari, and D. Zeppenfeld, Phys. Rev. D **68**, 073005 (2003).
 - [17] J. Campbell and R. K. Ellis, Phys. Rev. D **65**, 113007 (2002).
 - [18] M. Dührssen, ATLAS note ATL-PHYS-2003-030 (unpublished); Higgs Working Group Collaboration, K. A. Assamagan *et al.*, hep-ph/0406152.
 - [19] S. Catani and M. H. Seymour, Nucl. Phys. **B485**, 291 (1997); **B510**, 503(E) (1997).
 - [20] J. Pumplin, D. R. Stump, J. Huston, H. L. Lai, P. Nadolsky, and W. K. Tung, J. High Energy Phys. 07 (2002) 012.
 - [21] R. P. Kauffman, S. V. Desai, and D. Risal, Phys. Rev. D **55**, 4005 (1997); **58**, 119901(E) (1998).
 - [22] V. Del Duca, W. Kilgore, C. Oleari, C. Schmidt, and D. Zeppenfeld, Nucl. Phys. **B616**, 367 (2001).
 - [23] J. Campbell, R. K. Ellis, and D. Rainwater, Phys. Rev. D **68**, 094021 (2003).
 - [24] S. Catani, D. de Florian, and M. Grazzini, J. High Energy Phys. 05 (2001) 025.
 - [25] R. V. Harlander and W. B. Kilgore, Phys. Rev. D **64**, 013015 (2001).
 - [26] R. V. Harlander and W. B. Kilgore, Phys. Rev. Lett. **88**, 201801 (2002).
 - [27] C. Anastasiou and K. Melnikov, Nucl. Phys. **B646**, 220 (2002).
 - [28] V. Ravindran, J. Smith, and W. L. van Neerven, Nucl. Phys. **B665**, 325 (2003).
 - [29] E. L. Berger and J. W. Qiu, Phys. Rev. D **67**, 034026 (2003).
 - [30] E. L. Berger and J. W. Qiu, Phys. Rev. Lett. **91**, 222003 (2003).
 - [31] V. Ravindran, J. Smith, and W. L. Van Neerven, Nucl. Phys. **B634**, 247 (2002).
 - [32] S. Asai *et al.*, hep-ph/0402254.
 - [33] D. Cavalli *et al.*, ATLAS Internal Note PHYS-NO-051 1994 (unpublished).